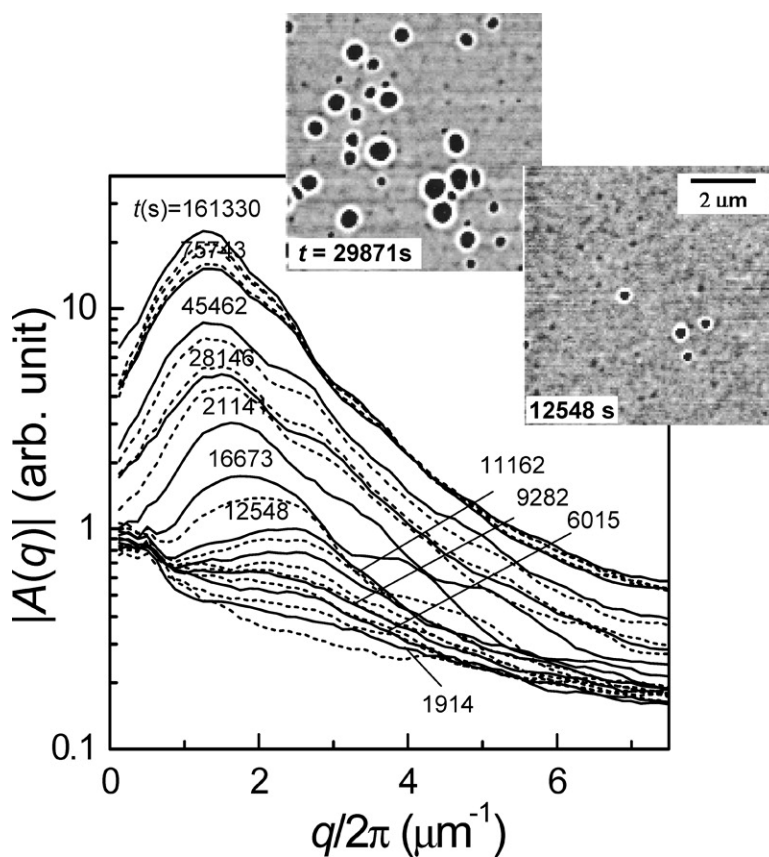


Unconventional Spinodal Surface Fluctuations on Polymer Films

Y. J. Wang, and Ophelia K. C. Tsui

Langmuir, 2006, 22 (5), 1959-1963 • DOI: 10.1021/la052750yDownloaded from <http://pubs.acs.org> on November 25, 2008

More About This Article

Additional resources and features associated with this article are available within the HTML version:

- Supporting Information
- Links to the 2 articles that cite this article, as of the time of this article download
- Access to high resolution figures
- Links to articles and content related to this article



Langmuir

Subscriber access provided by BOSTON UNIV

- Copyright permission to reproduce figures and/or text from this article

[View the Full Text HTML](#)



ACS Publications
High quality. High impact.

Langmuir is published by the American Chemical Society, 1155 Sixteenth Street N.W.,
Washington, DC 20036

Unconventional Spinodal Surface Fluctuations on Polymer Films

Y. J. Wang and Ophelia K. C. Tsui*

Department of Physics and Institute of Nanoscience and Technology, Hong Kong University of Science and Technology, Clear Water Bay, Hong Kong

Received October 12, 2005. In Final Form: November 28, 2005

We study the temporal growth pattern of surface fluctuations on a series of spinodally unstable polymer films where the instability can be adjusted with the film thickness, h_0 . For the most unstable film studied (whose $|(h_0 - h_{sp})/h_{sp}| = 0.988$; h_{sp} is the thickness where the second derivative of the interfacial potential of the film equals zero), the growth rate function of the surface modes as a function of the wavevector fits well to the mean-field theory. When the film thickness is increased such that $|(h_0 - h_{sp})/h_{sp}| \leq 0.977$, the mean-field theory demonstrates marked disagreement with experiment, notwithstanding the provision of the known corrections from nonlinear effects and thermal noise. We show that the deviations arise from large-amplitude fluctuations induced by homogeneous nucleation, which are not considered in the conventional treatments.

According to phase-transition theories, off-critical systems with dimensionalities below the upper critical value of 6 would have the mean-field spinodal smeared and the mean-field predicted phase properties invalidated by thermal fluctuations near the spinodal.^{1–3} Although non-mean-field behaviors are expected on both sides of the spinodal for these cases, a majority of studies have focused on the limit of metastability. No systematic experiment is dedicated to the investigation of how the phase behavior may change on the unstable side. Here, we examine the effect of thermal fluctuations on the spinodal growth of the order parameter in a 2D unstable system—polystyrene (PS) deposited on Si covered with 106-nm-thick SiO_x .^{4,5} Results of PS films with thicknesses of $h_0 = 3, 5.5$, and 11 nm are reported. Given the theoretical spinodal thickness $h_{sp} = 243$ nm,⁶ $|(h_0 - h_{sp})/h_{sp}|$ values of the studied films are 0.988, 0.977, and 0.955.

In spinodal rupturing, the film roughens by spontaneous growth of the surface fluctuations, which can be regarded as the order parameter, and may be decomposed into a sum of Fourier components by mean-field theory^{10,13}

$$h(\mathbf{r}, t) - h_0 = \sum_{\mathbf{q}} e^{\Gamma(\mathbf{q})t} A(\mathbf{q}, 0) \exp(i\mathbf{q}\mathbf{r}) \quad (1)$$

where $i = \sqrt{-1}$, \mathbf{r} is a 2D position vector on the film, t is time, $A(\mathbf{q}, 0)$ is the amplitude of the component with wave vector \mathbf{q} at $t = 0$, and $\Gamma(\mathbf{q})$ is the growth rate. Implicit in eq 1 is the dynamic equation

$$\frac{dA(\mathbf{q}, t)}{dt} = \Gamma(\mathbf{q}) A(\mathbf{q}, t) \quad (2)$$

By adopting the lowest-order approximation to the energy of the film upon roughening, it can be shown that $\Gamma(\mathbf{q})$ is isotropic and given by^{10,13}

$$\Gamma(q) = -\frac{h_0^3}{12\eta} \left[\frac{\partial^2 G}{\partial h_0^2} q^2 + \gamma q^4 \right] \quad (3)$$

where $q \equiv |\mathbf{q}|$, $G(h_0)$ is the interfacial potential of the film that has an initial thickness of h_0 , and η and γ are the viscosity and surface tension of the polymer, respectively. Equation 3 can be written in the following compact form

$$\Gamma(q) = \Gamma_m \left[2 \left(\frac{q}{q_m} \right)^2 - \left(\frac{q}{q_m} \right)^4 \right] \quad (4)$$

with $q_m = \sqrt{-G''(h_0)/2\gamma}$ being the wave vector that maximizes $\Gamma(q)$ and $\Gamma_m = \Gamma(q_m)$. If the magnitude of the surface fluctuations is not small, then the next higher-order term of the film energy ($\partial^4 G / \partial h_0^4 (h(\mathbf{r}) - h_0)^4 / 4!$) may need to be added. It can be shown that it leads to the same form of $\Gamma(q)$ as given in eq 4, but with q_m and Γ_m normalized according to¹⁰

$$q_m = u q_m^{(0)} \quad (5)$$

and

$$\Gamma_m = u^4 \Gamma_m^{(0)} \quad (6)$$

with

$$u = \sqrt{1 + \frac{\partial^4 G / \partial h_0^4 \langle (h - h_0)^2 \rangle}{2\partial^2 G / \partial h_0^2}} \quad (7)$$

where $q_m^{(0)} = \sqrt{-G''(h_0)/2\gamma}$ and $\Gamma_m^{(0)} = \Gamma(q_m^{(0)})$ are the limits of q_m and Γ_m as $\langle (h(\mathbf{r}) - h_0)^2 \rangle$ and hence the higher-order correction approaches zero. Equations 5 and 6 show that q_m and Γ_m should display consistent variations as $\langle (h(\mathbf{r}) - h_0)^2 \rangle$ increases with time.

For the present system, $G(h_0)$ is usually assumed to be the van der Waals (vdW) potential,^{7–9} although alternative origins of $G(h_0)$ have been proposed.^{6,14} Because the time factor in eq 1

* Corresponding author. E-mail: phtsui@ust.hk.

- (1) Binder, K. *Phys. Rev. A* **1984**, *29*, 341.
- (2) Klein, W.; Unger, C. *Phys. Rev. B* **1983**, *28*, 445.
- (3) Wang, Z.-G. *J. Chem. Phys.* **2002**, *117*, 481.
- (4) Du, B.; Xie, F.; Wang, Y. J.; Yang, Z.; Tsui, O. K. C. *Langmuir* **2002**, *18*, 8510.
- (5) Tsui, O. K. C.; Wang, Y. J.; Zhao, H.; Du, B. *Eur. Phys. J. E* **2003**, *12*, 417.
- (6) Zhao, H.; Wang, Y. J.; Tsui, O. K. C. *Langmuir* **2005**, *21*, 5817.
- (7) Reiter, G. *Phys. Rev. Lett.* **1992**, *68*, 75.
- (8) Xie, R.; Karim, A.; Douglas, J. F.; Han, C. C.; Weiss, R. A. *Phys. Rev. Lett.* **1998**, *81*, 1251.
- (9) Seemann, R.; Herminghaus, S.; Jacobs, K. *Phys. Rev. Lett.* **2001**, *86*, 5534.
- (10) Wang, Y. J.; Tsui, O. K. C. *J. Non-Cryst. Solids.*, in press.
- (11) Wang, X. P.; Xiao, X.; Tsui, O. K. C. *Macromolecules* **2001**, *34*, 4180.
- (12) Herminghaus, S.; Jacobs, K.; Seemann, R. *Eur. Phys. J. E* **2001**, *5*, 531.
- (13) Vrij, A.; Overbeek, J. Th. *J. Am. Chem. Soc.* **1968**, *90*, 3074.

(14) Morariu, D.; Schaffer, E.; Steiner, U. *Phys. Rev. Lett.* **2004**, *92*, 156102.

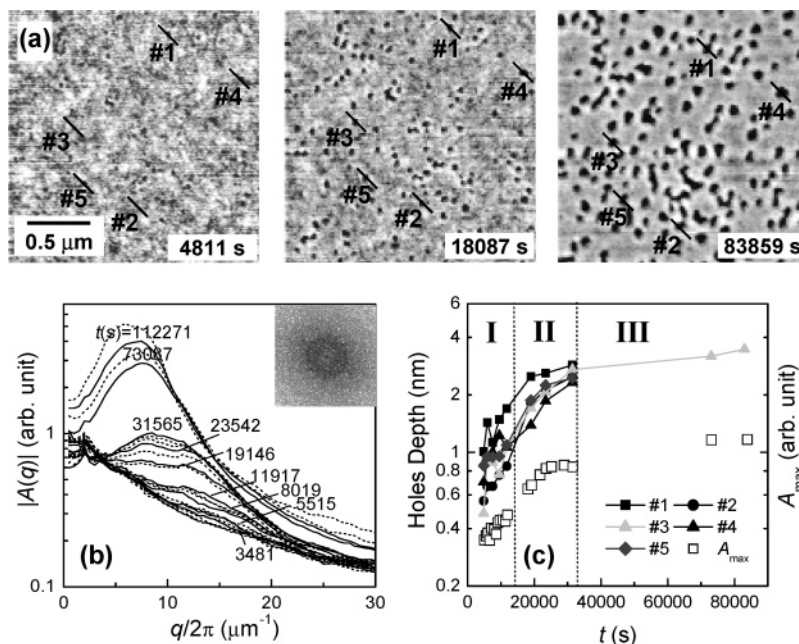


Figure 1. (a) AFM topographic images from a rupturing 3 nm film at the different values of t indicated. The scale bar on the first image applies to the other two images. (b) $|A(q)|$ of the same film plotted vs $q/2\pi$ at various values of t (indicated only for the spectra shown by solid lines). (Inset): 2D Fourier spectrum of the film after a ring is formed, where dark regions represent strong signals. (c) Simultaneous plots of A_{\max} and d_h vs t .

is exponential, the mode with $q = q_m$ quickly dominates, giving rise to a characteristic length equal to $2\pi/q_m$ in the film morphology and a ring with radius q_m in the 2D Fourier spectrum. For q greater than a cutoff of $\sqrt{2}q_m$, $\Gamma(q) < 0$ and the mode decays with time. The decay stems from the fact that the surface energy ($= \gamma|A(q)|^2q^2/2$) of the modes with $q > \sqrt{2}q_m$ is so large that the energy needed to create the mode becomes positive.¹⁰

Polystyrene homopolymer with molecular weight 2.3 kg/mol and polydispersity 1.07 was purchased from Scientific Polymer Products. Solutions of this polymer in toluene with different concentrations were prepared and spun-cast at 4000 rpm to produce PS films with the desired thickness. The SiO_x layer on the substrate was prepared by wet oxidation.¹¹ The thickness of the PS films and SiO_x was measured by ellipsometry. Topographic images of the films during rupture were acquired by a Seiko Instruments SPN3800 atomic force microscope (AFM) operated in noncontact mode in which the bright regions represent protrusions and the dark regions represent indentations. The annealing temperatures, being 32, 59, and 105 °C for the 3, 5.5, and 11 nm films, respectively, were chosen such that the rupture rate was convenient for the measurement. The fact that these temperatures are different has to do with the thickness dependence of the glass-transition temperature of this polymer film system.¹² By analyzing the temporal development of the radially averaged Fourier amplitude, $A(q, t) (\equiv \langle A(q, t) \rangle_{|q|=q})$, at each q , $\Gamma(q)$ can be determined.

Figure 1a shows three AFM images of a rupturing 3 nm film demonstrating its morphologic development in the early stage. It is apparent from Figure 1a that the growing surface fluctuations are correlated, as confirmed by the formation of a ring in the 2D Fourier spectrum of the images (inset of Figure 1b) and a peak in the radially averaged Fourier spectrum (main panel of Figure 1b) after ~ 3500 s. As seen from Figure 1b, $A(q)$ develops a peak at $q_m/2\pi \approx 11 \mu\text{m}^{-1}$ initially, which shifts to smaller q 's at later times, consistent with coarsening, and eq 5 with $\partial^4 G/\partial h_0^4 > 0$. Figure 1c displays the time variations of the peak height of $|A(q)|$, A_{\max} , and the depth, d_h , of five randomly selected holes marked in Figure 1a. As seen, $A_{\max}(t)$ increases exponentially with time

initially, in agreement with eq 1, but slows down after $t > 2.5 \times 10^4$ s. Interestingly, the evolution of d_h , which is identical for all five holes, closely follows that of A_{\max} . The plateau in d_h can be understood from d_h 's reaching h_0 , whereupon its growth is hindered by the bottom substrate. The exact correspondence between $d_h(t)$ and $A_{\max}(t)$ and the simultaneous growth of all five randomly selected holes strongly suggest that the deepening of the holes comes from the amplification of the spinodal surface fluctuations.

Figure 2 displays the corresponding results obtained from a rupturing 5.5 nm film. In contrast to the 3 nm film, the rupturing morphology here is dominated by irregularly scattered holes emerging at random times. Nevertheless, the Fourier spectrum (Figure 2b) still clearly shows a peak at ~ 6000 s. The initial peak position, occurring at $q_m/2\pi \approx 2.5 \mu\text{m}^{-1}$, does not correspond to any obvious length scale pertinent to the holes in the respective images. Compared to the value of $q_m/2\pi \approx 11 \mu\text{m}^{-1}$ found with the 3 nm film, the value obtained here is in reasonable agreement with the scaling $q_m \sim h^{-2}$ given the prevalent form of $G(h_0) \sim h_0^{-2}$, which is appropriate for nonretarded vdW interactions^{7,9} and confined phonon fluctuations.¹⁴ In Figure 2c, d_h of the five randomly selected holes defined in Figure 2a demonstrates growth rates close to that of the spinodal fluctuations initially but jumps into full-thickness holes at sporadic times. The random nature of the jump-in of the holes and a calculation⁵ showing that the opening of the holes can involve activation barriers comparable to $k_B T$ have led us to postulate that holes are due to thermal nucleation.⁵ Figure 2c also shows that A_{\max} versus t displays an upturn near the time when the initial jump-in of holes takes place. An upturn in $A_{\max}(t)$ can potentially be explained by the increase in $-G''(h)$ as the holes deepen. Assuming the prevalent form, $G(h) \sim h^{-2}$, the fractional change in $-G''(h)$ ($\equiv (G''(h) - G''(h_0))/G''(h_0)$) is $\sim (6(h-h_0)^2/h_0^2)$. Therefore, any resultant acceleration in the growth rate should appear sooner with thinner films, but an upturn in $A_{\max}(t)$ is found only in the two thicker films. In fact, given q_m to be decreasing with time (Figure 2b), an upturn in $A_{\max}(t)$ is inconsistent with the mean-field predictions (eqs 5–7) from higher-order corrections.

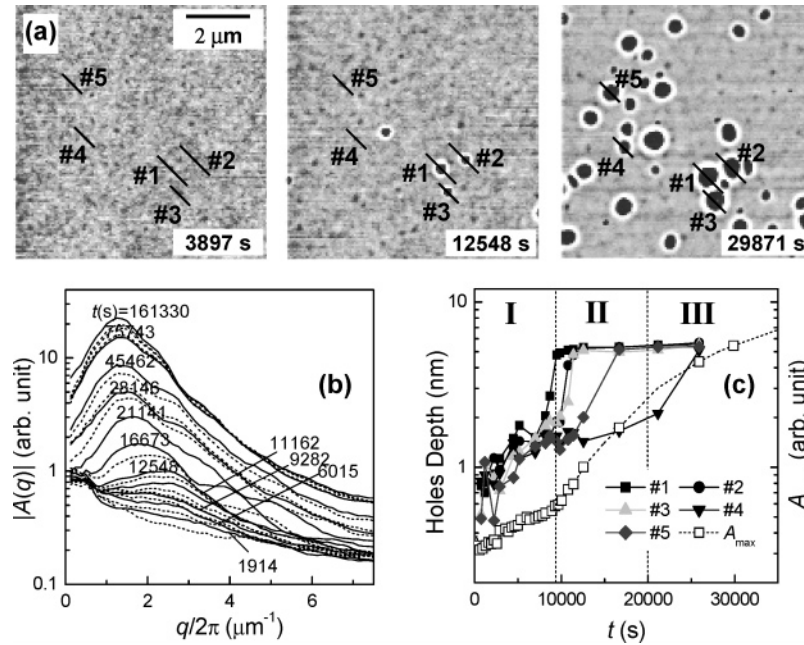


Figure 2. (a) AFM topographic images from a rupturing 5.5 nm film at the different values of t indicated. The scale bar applies to all three images. (b) $|A(q)|$ of the same film plotted vs $q/2\pi$ at various values of t (indicated only for the spectra shown by solid lines). (c) Simultaneous plots of A_{\max} and hole depth vs t .

In Figure 3a and b, we have plotted the growth rate function, $\Gamma(q)$, of the 3 and 5.5 nm films in different time zones as defined in Figures 1c and 2c, respectively. The solid lines are fits to eq 4. For the 3 nm film, the data of all three time zones display good fits although the experimental cutoff wavelengths in time zones II and III occur at notably smaller values than predicted. The occurrence of the short-wavelength cutoff at a smaller-than-predicted value is commonplace and well documented.^{10,15,16} It arises from stochastic thermal agitations providing the energy required to excite the $q > \sqrt{2}q_m$ modes that would otherwise be decaying.¹⁰ Therefore, the entire rupturing of this film demonstrates excellent agreement with the mean-field theory. For the $\Gamma(q)$ data of the 5.5 nm film, however, only the points obtained in time zone I fit well to the model. Data obtained in time zone II, fitting marginally to eq 4, demonstrate growth rates that are far above those in time zone I, in keeping with the upturn of $A_{\max}(t)$ shown in Figure 2c. However, the position of the peak is essentially unchanged. The independence of the growth rate on q_m is a strong indication that the growth dynamics in time zone II is not spinodal. The $\Gamma(q)$ data obtained in time zone III is essentially flat, showing no peak or a short-wavelength cutoff, which is also unlike the spinodal.

We examine a still thicker film with thickness equal to 11 nm. Shown in Figure 4a are three AFM images of the film representing its rupturing. As seen, there are growing fluctuations on the film surface from the beginning. At $t \approx 2700$ s, the first hole appears whereupon more holes emerge with time. The data of A_{\max} vs t (Figure 4b) reveal additional details. The growth of the surface fluctuations actually slows down after ~ 600 s but begins to accelerate at ~ 2500 s, which, interestingly, coincides with the time when the first hole appears. To see if this upturn is connected with the emergence of the holes, we carefully select a smaller area inside the whole image where no holes appear and reanalyze A_{\max} versus t . The result, plotted as open circles in Figure 4b, shows that the upturn disappears.

We seek further evidence that the upturn has non-mean-field character. Shown in Figure 5a are the corresponding regional

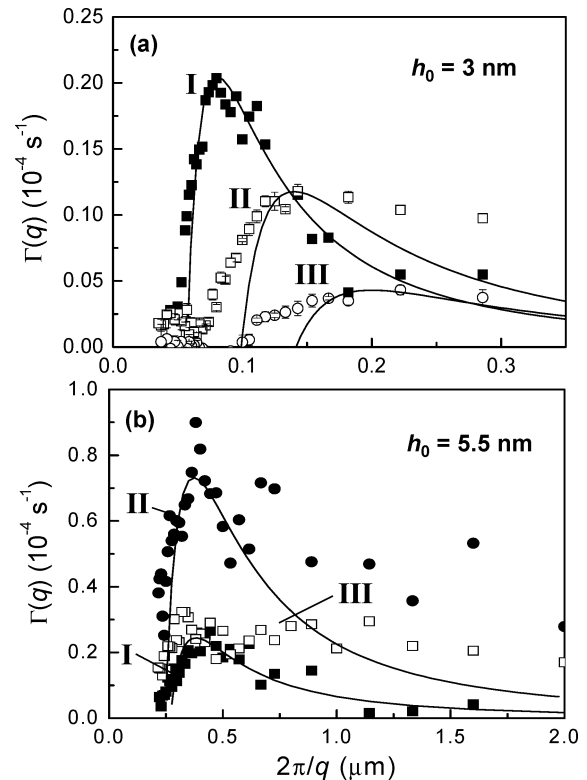


Figure 3. $\Gamma(q)$ function of (a) 3 and (b) 5.5 nm films in different time zones defined in Figures 1c and 2c, respectively. Solid lines are fits to eq 4.

and time-sequenced data of $\Gamma(q)$ of the 11 nm film. Before the onset of the upturn (i.e., time zones I and II), the $\Gamma(q)$'s of the whole image and the no hole area look alike, consistent with the good agreement displayed by the respective $A_{\max}(t)$'s in these time zones (Figure 4b). After the upturn, A_{\max} in the whole image increases 10-fold within time zone III, but the corresponding increase in A_{\max} in the no holes area is only 2-fold. A consistent difference is found in the maximum of $\Gamma(q)$ displayed in Figure

(15) Langer, J. S.; Bar-on, M.; Miller, H. D. *Phys. Rev. A* **1975**, *11*, 1417.
(16) Cook, H. E. *Acta Metall.* **1970**, *18*, 297.

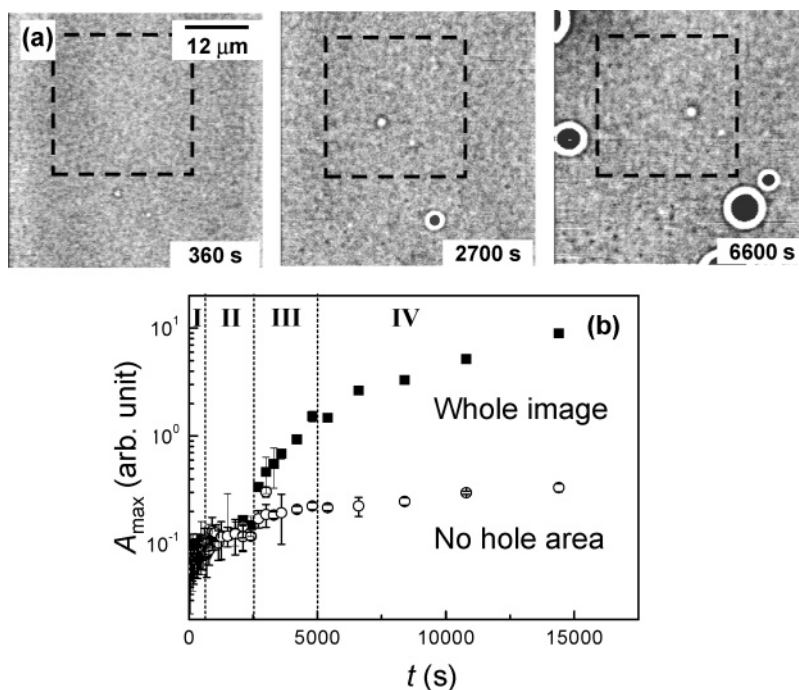


Figure 4. (a) AFM images obtained from a rupturing 11 nm film at the different values of t indicated. The area framed by dashed lines is selected to contain no hole and is termed the no hole area in the text. (b) Plots of A_{\max} vs t from data of the whole image and the no hole area shown in part a.

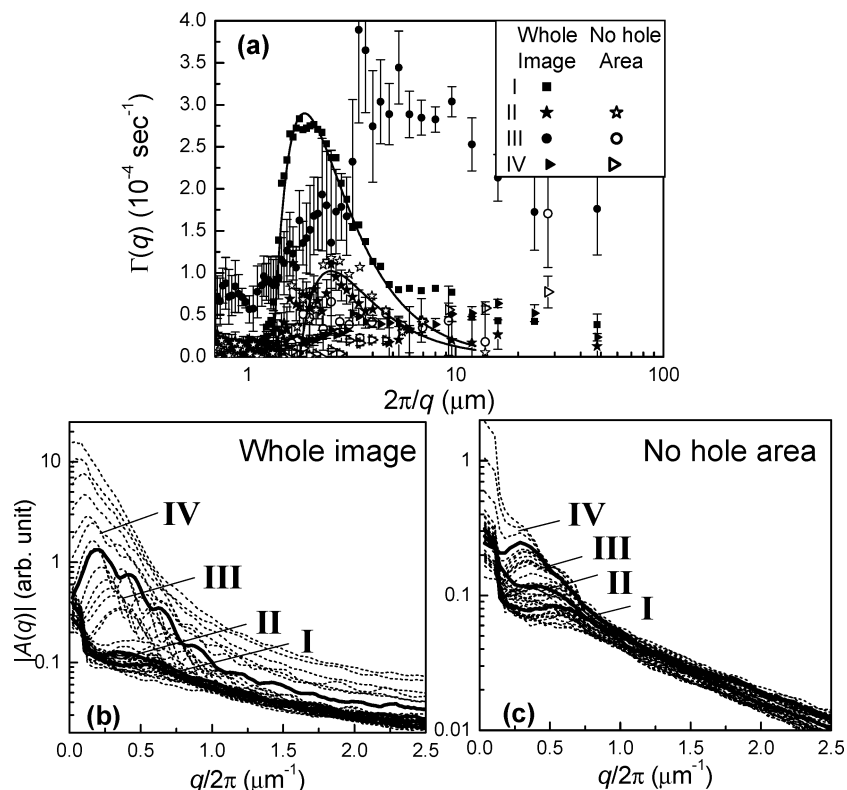


Figure 5. (a) $\Gamma(q)$ function deduced from the whole image and the no hole area of the same film shown in Figure 4b at different time zones. Solid lines are fits to eq 4. (b) $|A(q)|$ vs $q/2\pi$ from the whole image and (c) the no hole area at various values of t (indicated for the curves shown by solid lines).

5a. All of these illustrate the good corroboration between the data of $A_{\max}(t)$ and $\Gamma(q)$'s in different time zones. The most striking observation is that despite the notable rise in $\Gamma(q)$ for the whole image after the upturn (Time zone III, Figure 5a) q_m , in contrast, displays a factor of 2 reduction, and this takes place after $\Gamma(q)$ has demonstrated standard mean-field coarsening (i.e., a simultaneous reduction in q_m and Γ_m with time; time zone II).

We further notice that unlike the short-wavelength modes in the no hole area those in the whole image demonstrate substantial growth showing no sign of a cutoff. This difference is readily recognizable by comparing the Fourier spectra of the whole image with those of the no hole area: In the former, the growth of $|A(q)|$ is still substantial (Figure 5b), but in the latter, only a small change in $|A(q)|$ occurs in the large q region (Figure 5c).

The lack of a cutoff in $\Gamma(q)$ after the upturn is another indication of non-mean-field behavior.

The influence of stochastic thermal noise on the dynamics of spinodal decomposition has been treated.^{10,15,16} By adding a random force term of $q^2\xi(\mathbf{q}, t)$ (where $\langle \xi(\mathbf{q}, t) \xi(\mathbf{q}, t') \rangle = 2|\Theta(\mathbf{q})|^2\delta(t - t')$) to the dynamic eq 2, it is straightforward to show that the solution for $|A(q, t)|^2$ is modified to^{16,17}

$$|A(q, t)|^2 = \left\{ |A(q, 0)|^2 + \frac{q^4|\Theta(\mathbf{q})|^2}{\Gamma(q)} \right\} \exp[2\Gamma(q)t] - \frac{q^4|\Theta(\mathbf{q})|^2}{\Gamma(q)} \quad (8)$$

And correspondingly, the dynamic equation of $|A(q, t)|^2$ is changed to

$$\frac{d|A(q, t)|^2}{dt} = 2\Gamma(q)|A(q, t)|^2 + 2q^4|\Theta(\mathbf{q})|^2 \quad (9)$$

If $\Gamma(q)$ is negative, then eq 8 describes how an out-of-equilibrium system is restored to the equilibrium spectral power density, $|A(q, \infty)|^2$, by thermal noise. This consideration enables us to identify $2q^4|\Theta(\mathbf{q})|^2$ with $2|\Gamma(q)||A(q, \infty)|^2$. The absolute sign of $\Gamma(q)$ ensures that $q^4|\Theta(\mathbf{q})|^2$ is always positive and hence allows the identification to be generalized to cases where $\Gamma(q) > 0$. By assuming the Boltzmann distribution for the surface fluctuation modes, one obtains $2q^4|\Theta(\mathbf{q})|^2 = h_0^3k_B Tq^2/6\eta$, which is independent of $G(h(\mathbf{r}) - h_0)$ and hence any approximation assumed thereof. By incorporating the higher-order corrections to $\Gamma(q)$, one recovers Langer's nonlinear equation of motion for $|A(q, t)|^2$ (i.e., eq 2.9 of ref 15). Provided $\Gamma(q)$ is normalized for the nonlinear corrections, eqs 8 and 9 are applicable to any arbitrary starting time, t_0 .

Here, we are interested in the spinodal unstable case where $\Gamma(q) > 0$. The random force discussed above causes the apparent growth rate, $\Gamma_{\text{apparent}}(q) \equiv (1/2t)\ln|A(q, t)/A(q, t_0)|^2$, to be larger than the intrinsic growth rate, $\Gamma(q)$. By applying eq 8, $\Gamma(q)$ is related to the measured values of $|A(q, t)|^2$ according to

$$\Gamma(q) = \frac{1}{2t} \ln \left\{ \frac{|A(q, t)|^2 + |A(q, \infty)|^2}{|A(q, t_0)|^2 + |A(q, \infty)|^2} \right\} \quad (10)$$

Here, t is measured from some reference time, t_0 . By using eq 10 and assuming $|A(q, t_0)/A(q, \infty)|^2 \ll 1$, one finds

$$\frac{\Gamma_{\text{apparent}}(q)}{\Gamma(q)} \approx \frac{1}{t'} \ln \left\{ \left[\frac{|A(q, \infty)|^2}{|A(q, t_0)|^2} \right]^2 [\exp(t') - 1] \right\} \quad (11)$$

where $t' \equiv 2\Gamma(q)t$. By adopting $t' = 1$ and $|A(q_m, t_0)/A(q_m, \infty)|^2 \approx [h_{\text{rms}}(t_{\text{upturn}})/h_{\text{rms}}(\infty)]^2 \approx [h_{\text{rms}}(t_{\text{upturn}})/h_0]^2$, which is found to be 0.064 and 0.022 for the 5.5 and 11 nm films, respectively, in eq 11, with t_{upturn} being the time when the upturn in $A_{\text{max}}(t)$ appears and $h_{\text{rms}}(t)$ being the rms roughness of the film at time t , we

estimate that $\Gamma_{\text{apparent}}(q)/\Gamma(q) = 6.0$ and 8.9 for the $h_0 = 5.5$ and 11 nm films, respectively. This result can account very well for the noted factor of 3 rise in $\Gamma(q_m)$ after the upturn (Figures 3b and 5c). We remark that the effect of thermal fluctuations treated here on the growth of the spinodal fluctuations is different from the conventional treatment,¹⁵⁻¹⁷ in which $|A(q, \infty)|^2$ is taken to be $k_B T / (G''(h) + \gamma q^2)$ and hence varies as the film surface $h(\mathbf{r})$ evolves. This approximation would be invalidated if the stochastic thermal fluctuations are large enough to facilitate the film's access to the true equilibrium configuration within a short time of $\sim 1/\Gamma_m$. Assuming the equilibrium configuration to be an abrupt, full-thickness hole, $|A(q, \infty)|^2$ would be h_0^2 . Nonetheless, for most systems studied in the past, the conventional treatment has provided an excellent account of the commonly found deviations between theory and experiment. These deviations, including the larger-than-expected values of the measured cutoff wavevector in $\Gamma(q)$ and the growth rate of the modes with q far removed from q_m , are also found in the 3 nm film (Figure 3a) and appear at the beginning of the spinodal process. However, the deviations found in the 5.5 and 11 nm films due to the upturn appear only after some time delay. This suggests that the mechanism instigating the upturn obliges the system to overcome some energy barriers. This characteristic distinctively matches that of thermal nucleation.

In conclusion, we have observed unconventional deviations from mean-field theory in the growth pattern of spinodal surface fluctuations of polymer films, most notably the upturn in $A_{\text{max}}(t)$, which we establish to arise from thermal nucleation. Because our discussions are general, the same irregularities should be present in any phase-separation processes where the thermal noise induces large-amplitude order parameter fluctuations comparable to those at equilibrium. This condition coincides with the Ginzburg criterion suggested by Binder¹ for the invalidation of the mean-field theory in the spinodal region. Our result shows that the large-amplitude fluctuations occurs by way of homogeneous nucleation. It is remarkable that these large-amplitude fluctuations begin to appear in the present system quite deep in the unstable region, namely, where $|(h_0 - h_{\text{sp}})/h_{\text{sp}}|$ is only 2.3% below one. Recently, Bollinne et al.¹⁸ reported unconventional spinodal-like rupturing of 15-nm-thick PS films on silicon that are theoretically metastable. The two observations reveal an unprecedented broadening in the transition from unstable to metastable phase behavior in thin films. The most probable cause of the extraordinary broadening is that the dimensionality of thin films, being two, is well below the upper critical dimension of six. Under this condition, the mean-field predicted phase properties, such as the spinodal, can be easily destroyed by thermal fluctuations.

Acknowledgment. We thank C. H. Lam, T. K. Ng, and P. M. Chaikin for useful discussions. This work is supported by the Research Grant Council of Hong Kong through projects HKUST6070/02P and 603604.

LA052750Y

(17) In ref 16, we find a negative sign missing from the exponential in the equation after eq 17 and all of the terms involving $Q(k)$ between eqs 18 and 21.

(18) Bollinne, C.; Cuenot, S.; Nysten, B.; Jonas, A. M. *Eur. Phys. J. E* **2003**, *12*, 389.